ECMWF Feature article

from Newsletter Number 146 – Winter 2015/16

METEOROLOGY

Reducing systematic errors in cold-air outbreaks

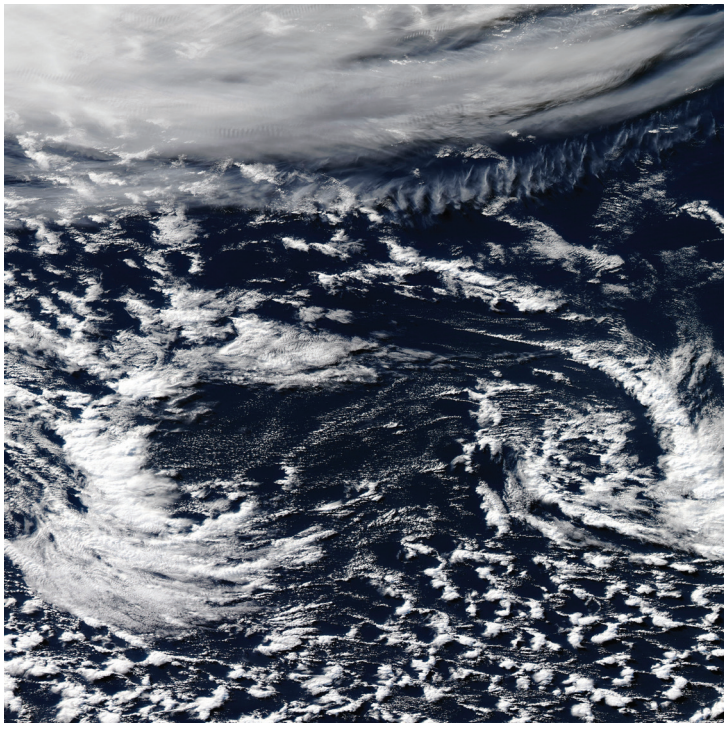

NASA Worldview

www.ecmwf.int/en/about/news-centre/media-resources

doi: 10.21957/s41h7q7l

This article appeared in the Meteorology section of ECMWF Newsletter No. 146 – Winter 2015/16, pp. 17–22.

Reducing systematic errors in cold-air outbreaks

Richard Forbes, Alan Geer, Katrin Lonitz, Maike Ahlgrimm

Models and observations both have uncertainties. Characterising and representing uncertainty and its growth in time is a significant activity at ECMWF with the development of ensemble forecasts (ENS) and more recently the Ensemble of Data Assimilations (EDA). At the same time, an ongoing challenge of research and development is to reduce uncertainties in both the initial state and the forecast model through improvements in the use of observations, data assimilation methodologies and the fidelity of the model dynamics and physics.

Comparing model forecasts with observations on medium-range to seasonal timescales can highlight systematic errors, but non-linear interactions and feedbacks make it difficult to attribute the errors to a particular source. Using short-range forecasts in the data assimilation system, on the other hand, means the model state is reasonably close to reality, and systematic departures of these forecasts from the observations are more easily assessed. Such assessments may even make it possible to identify regime-(or flow-)dependent systematic errors and to attribute these errors to specific physical processes.

In this article, we describe how this approach has enabled us to identify supercooled liquid water cloud in convective cold-air outbreaks as the source of regime-dependent systematic model errors in simulated microwave radiance and shortwave radiation. A proposed solution reduces the model errors at all forecast lead times. This is seen in reduced bias against assimilated microwave observations and reduced shortwave radiation error.

All-sky microwave radiance errors

The first part of the tale is about diagnosing systematic model errors using the data assimilation scheme in ECMWF's Integrated Forecasting System (IFS). Data assimilation combines the model with observations in an optimum analysis of the atmospheric state that is better than either the model or observations on their own. It is designed to minimise random errors, but there are also many systematic differences between models and observations. In practice, such differences are removed by the observational bias correction process, but if the model bias is too large it is better not to assimilate the affected observations. These systematic differences deserve careful study: whether they are associated with the model, the observation operator, or the observations, they indicate a scientific problem that needs fixing at source.

Microwave imager radiances in clear, cloudy and precipitating conditions (also known as all-sky conditions) have been assimilated operationally into the IFS since 2009 (*Bauer et al.*, 2010). Typical instruments like the Special Sensor Microwave Imager/Sounder (SSMI/S, see Box A) measure a range of frequencies with strong sensitivities to atmospheric water vapour, rain, snow and liquid water cloud. Differences between the observations and a short-range forecast (0–12 hours) within each assimilation cycle are called first-guess departures. A forward operator calculates the predicted microwave radiance brightness temperatures from the model geophysical fields to compare directly with the observations. The first-guess departures can be a valuable source of information on systematic model errors, or 'biases'. However, because they are expressed in radiance terms and because the radiances are affected by a range of atmospheric and surface parameters, it can sometimes be difficult to attribute these departures to a particular cause.

Figure 1a shows the annual mean first-guess departures for the SSMI/S 92 GHz microwave radiance brightness temperature for the operational IFS high-resolution model (HRES) for 2014–2015 over the oceans. Significant positive differences are apparent towards the polar side of the extra-tropical storm track in the southern and northern hemispheres as well as in the maritime stratocumulus regions off the coast of South America and Africa, and to a smaller extent along the inter-tropical convergence zone (ITCZ) over the Pacific Ocean.

The extra-tropical storm track brightness temperature departures have been a long-standing difficulty when assimilating the microwave imagers in all-sky conditions. Since systematic first-guess departures can degrade the analysis, the observations involved have had to be screened out. Several years ago significant first-guess departures were found to be associated with cold dry air moving equatorward behind cold fronts in the winter hemisphere (*Geer & Bauer*, 2010). These are regions where convection is active due to the instability produced by cold air flowing over the warmer ocean and where positive departures for certain microwave frequency brightness temperatures were often 5 to 10 K. Due to the low water vapour in these cold air masses in the model and the insensitivity of these microwave frequencies to cloud ice particles,

 doi:10.21957/s41h7q7l

a lack of cloud liquid water in the model is the most obvious explanation for the problem. Although targeted screening of the observations in these regions can avoid degrading the analysis (*Lonitz & Geer*, 2015), a more desirable approach is to improve the model physics to reduce the first-guess departures and be able to assimilate these observations.

Satellite observations

A

Microwave radiometer SSMI/S

The Special Sensor Microwave Imager/Sounder (SSMI/S) is a passive microwave radiometer on board a series of Defense Meteorological Satellite Program (DMSP) near- polar-orbiting satellites. The SSMI/S instrument measures microwave radiance at 24 discrete frequencies from 19 to 183 GHz with di erent sensitivities to atmospheric temperature, water vapour, rain, cloud liquid water, and at higher frequencies also cloud ice and frozen particles. The 37 and 92 GHz channels are particularly sensitive to vertically integrated cloud liquid water.

CERES shortwave and longwave radiation

The Clouds and the Earth's Radiant Energy System (CERES) instrument passively measures both the solar-re ected and Earth-emitted radiation from the atmosphere. There are instruments on board a number of polar-orbiting satellites (Aqua, Terra, NPP) providing global coverage in a 24-hour period.

MODIS visible image

The Moderate Resolution Imaging Spectroradiometer (MODIS) passively measures electromagnetic radiation across a wide spectrum and is on board both the NASA Terra and Aqua polar-orbiting satellites, completely observing the whole globe in 1 to 2 days. The true-colour image combines the red (670 nm), green (565 nm) and blue (479 nm) channels to create a view similar to that which would be seen by the human eye.

CloudSat and CALIPSO

CloudSat and CALIPSO are near-polar-orbiting satellites carrying a 94 GHz radar and a multi-frequency (532/1064 nm) lidar, respectively. Both instruments are active in the sense that they emit a signal and measure the backscatter from the atmosphere, clouds and precipitation. The lidar signal is strongly attenuated by small cloud droplets, enabling the identi cation of liquid water layers near cloud top at any temperature.

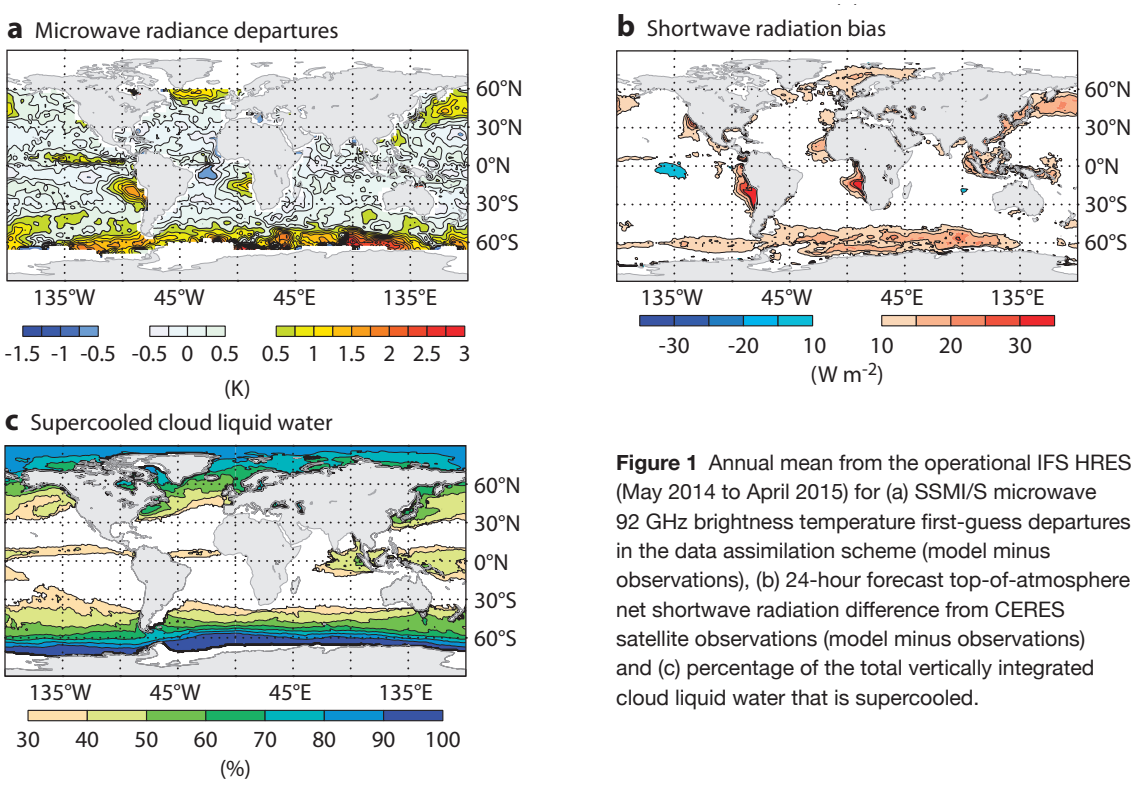

Figure 1 Annual mean from the operational IFS HRES (May 2014 to April 2015) for (a) SSMI/S microwave 92 GHz brightness temperature first-guess departures in the data assimilation scheme (model minus observations), (b) 24-hour forecast top-of-atmosphere net shortwave radiation difference from CERES satellite observations (model minus observations) and (c) percentage of the total vertically integrated cloud liquid water that is supercooled.

Shortwave radiation errors

The second part of this tale is the long-standing systematic error in the global shortwave radiation field. The top-of-atmosphere radiation is a direct well-observed quantity globally available from polar-orbiting and geostationary satellites and is an important metric for evaluating models across a wide range of space and timescales. In particular, the reflected shortwave radiation is significantly affected by the surface albedo and by cloud. Shortwave radiation errors in the IFS are routinely evaluated at ECMWF and show an improvement over the last decade due to a better representation of cloud as well as surface albedo. However, there are certain long-standing systematic errors in the shortwave radiation that continue to be present in the IFS at all forecast time ranges and model resolutions, suggesting deficiencies in the representation of cloud-related physical processes.

Figure 1b shows the annual mean top-of-atmosphere net shortwave radiation bias over the oceans in HRES for 2014–2015. The largest signal is from the subtropical marine stratocumulus regions in the eastern part of major oceanic gyres. However, there is also a significant positive shortwave radiation bias centred around ±60° latitude in the northern and southern hemisphere storm tracks over the North Atlantic, North Pacific and Southern Ocean, similar to the pattern of microwave radiance bias seen in Figure 1a. The storm-track errors are the focus of this article, but both the maritime stratocumulus and higher-latitude signals are consistent with either too little cloud cover, too little cloud water path, or incorrect optical properties, leading to not enough reflection back to space and too much radiation reaching the surface. Similar systematic errors are present at all resolutions of the IFS and at all forecast lead times out to seasonal timescales (as will be shown later). In addition, similar errors can be seen in many other numerical weather prediction (NWP) and climate models, so the problems are not specific to the IFS.

Supercooled liquid water cloud

We next explore the potential link between the systematic model errors seen in the shortwave radiation and the suggestion, based on microwave radiance observations, that in some situations the vertically integrated cloud liquid water in the model is too low. At the latitudes of the northern and southern hemisphere storm tracks, the temperature of the cloud top is often below 0°C. Figure 1c shows the global annual mean distribution of the percentage of the vertically integrated cloud liquid water content that is supercooled (i.e. the proportion of cloud liquid water at temperatures colder than 0°C). The data is again from the operational HRES for 2014–2015. Supercooled liquid water (SLW) has a significant presence in the mid-latitude storm tracks in both hemispheres, with 50–100% of cloud liquid being supercooled in the region of the shortwave radiation and SSMI/S brightness temperature biases. There is a seasonal shift north and south corresponding to the seasonal cycle (not shown). Although this is a model estimate, these regions with significant supercooled water in the IFS are consistent with the spatial distribution of supercooled liquid water occurrence observed from satellite lidar (*Hu et al.*, 2010), which is particularly sensitive to small liquid water drops at cloud top.

Based on previous studies, we also know that supercooled liquid water has a significant impact on the reflection of shortwave radiation, particularly when it is present at cloud top. The microwave radiance assimilation suggests a lack of cloud liquid water in the areas of convective cold-air outbreak, and these regions are also where the cloud is mostly colder than 0°C. The overall hypothesis is therefore that it is a lack of supercooled liquid water at cloud top in the convective cells associated with cold-air outbreaks that is the cause of the errors in both microwave radiances and the shortwave radiation.

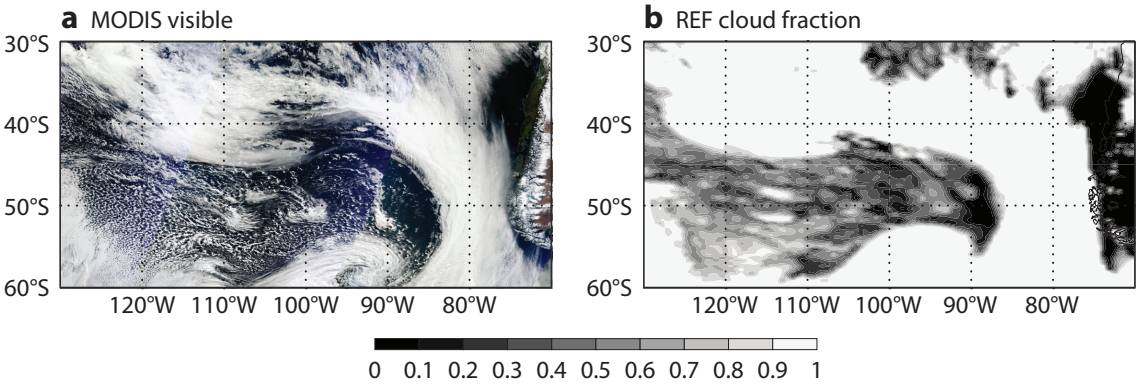

Figure 2 (a) MODIS visible image for approximately 12 UTC on 24 August 2013 and (b) 12-hour forecast of cloud fraction from the reference IFS (REF) valid at 12 UTC.

doi:10.21957/s41h7q7l

A regime-dependent systematic error

We focus on one particular day during August 2013 in the southern hemisphere storm track to illustrate the relationship between different variables and diagnose the specific model error (note that we could have chosen any number of days which show similar features). Figure 2a shows the MODIS visible image (Box A) for a region to the west of South America between 60°S and 30°S (70°W–130°W) valid for around 12 UTC on 24 August 2013. This region is characterised by a deep frontal cloud band in the eastern half of the domain, bending towards the west in the northern part of the domain. In the south-western quadrant there is a region of convective cells, where cold air is flowing equatorward from the Antarctic ice sheet over the warmer water of the Southern Ocean behind the front. The warmer ocean provides the instability to produce convection over a large region in what is often known as a cold-air outbreak.

Figure 2b shows the total cloud cover from an IFS 12-hour forecast (reference forecast, REF) valid at approximately the same time as the MODIS image. The short-range model forecast is close to the analysis and accurately captures the locations and variations of the different cloud regimes, from the overcast frontal cloud to the broken cloud cover associated with the convective cold-air outbreak behind the front.

Figure 3a shows the corresponding vertically integrated total liquid water path (LWP) from REF, highlighting the high liquid water content associated with the frontal band and smaller LWP associated with warm-phase low-level cloud in the north of the domain. However, there is an almost complete absence of liquid water in the region of cold convection, where the cloud in the model is present but essentially all ice.

The CloudSat and CALIPSO satellites with radar and lidar instruments passed across the region of cold-air convection later that same day. A vertical cross section showing cloud phase obtained from radar/lidar data (Box A) from 70°S to 30°S is shown in Figure 4a. The flow is from the south (left-hand side of the figure) and shows the growth of the mixed-phase cloud-topped boundary layer due to increasing surface heat fluxes from the warmer ocean below. There is a transition to convection at about 60°S. The 0°C isotherm from the model shows that all the liquid near the top of the boundary layer cloud to the south of 40°S is supercooled. Note the presence of supercooled water in the cold-air convection at cloud top between 60°S and 50°S with temperatures below –20°C. Note also that the radar/lidar combination will only be able to observe liquid water close to cloud top so there is more uncertainty in the cloud phase lower in the cloud. Figure 4b shows the cloud phase for the IFS equivalent to the observed cross section. The cloud phase is calculated by simulating the satellite track and radar/lidar signals in the model and is therefore a comparable product to the observations. The lack of any significant supercooled water is evident between about 60°S and 45°S.

The first-guess departure for SSMI/S 92 GHz microwave radiance brightness temperature in the analysis valid for the same date and time at 12 UTC is shown in Figure 3c. The observations suggest this lack of supercooled liquid in the convective region is a real deficiency of the model, with positive departures of 5–10 K. There are also large brightness temperature departures associated with the frontal cloud band, but these are more randomly distributed with adjacent positive and negative values associated with slight displacements of the front and small-scale uncertainties.

The final piece to complete the picture is the shortwave radiation bias, which is shown in Figure 3e. The figure shows the IFS shortwave radiation bias over the 24-hour period centred on 12 UTC on the same day, using observations from the daily average CERES dataset compiled from multiple satellite sources (Box A). These observations show there is too little radiation being reflected back to space in the cold-convective region, where there is also negligible supercooled cloud water in the model.

This same pattern of correlated errors in supercooled liquid water and shortwave radiation is repeated over and over in the convective cold-air outbreak regime in both the southern and northern hemispheric storm track, and it can explain the mean errors in the shortwave radiation in the IFS. The reason the error is dominant in the southern hemisphere is due to the high occurrence of the cold-air convection regime over the Southern Ocean. Modifying the physical process parametrizations that affect cloud phase should therefore lead to a reduction of the error in both hemispheres.

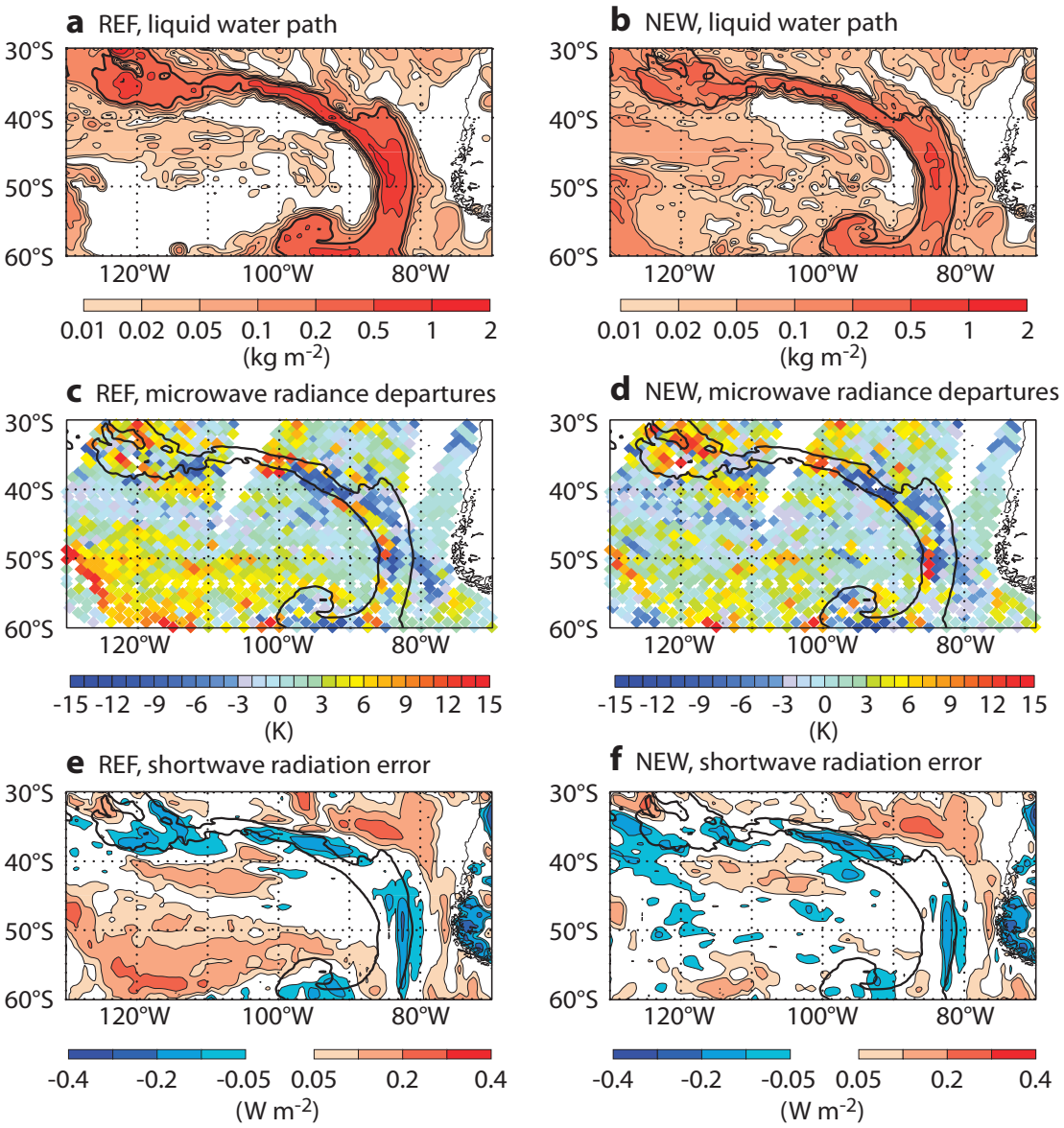

Figure 3 Model fields for 24 August 2013 for the reference IFS (REF; left-hand column) and the IFS with modified convective supercooled liquid water detrainment (NEW; right-hand column) showing (a, b) total liquid water path at 12 UTC from a 12-hour forecast, (c, d) SSMI/S 92 GHz brightness temperature first guess departure in the 12 UTC analysis and (e, f) 24-hour forecast averaged net top-of-atmosphere shortwave radiation difference from observations (IFS – CERES).

doi:10.21957/s41h7q7l

Reducing the error

Supercooled liquid water cloud is a challenge to represent in large-scale models because its presence is dependent on a balance of many processes. These include small-scale turbulent production of water saturation; ice nucleation and subsequent ice particle growth through water droplet evaporation (the Wegener-Bergeron-Findeisen process); and riming (falling ice particles collecting and freezing supercooled water droplets). There are therefore many uncertainties in parametrizing these processes in atmospheric models for both stratiform and convective cloud.

Before the end of 2010, the IFS represented mixed-phase cloud with a fixed global diagnostic temperature-dependent function. This meant that cloud was considered to be all liquid for temperatures warmer than 0°C, all ice for temperatures colder than –23°C, and a decreasing proportion of supercooled liquid water in between. A similar diagnostic approach to partitioning cloud phase has been common in global models with relatively simplified microphysics parametrization and is designed to be a first approximation to the global average occurrence of supercooled liquid water. However, in reality condensate in a cloud at a particular location and given temperature (say –10°C) can be all supercooled liquid or all ice depending on the history of the cloud and its environment.

In November 2010, a new cloud scheme was introduced in the IFS with separate predicted variables for cloud ice and cloud liquid and a more physical parametrization of mixed-phase microphysical processes (*Forbes & Tompkins*, 2011), allowing an improved representation of supercooled liquid water for stratiform cloud (*Forbes & Ahlgrimm*, 2014). However, the convection parametrization retained the fixed diagnostic temperature-dependent function, with all liquid at 0°C changing to all ice at –23°C. It is the convective mixed phase that is the relevant process in this study.

As seen in the cross section in Figure 4a, the cloud top in the convective cold-air outbreaks, identified as the problem regime, can often be colder than –20°C. Whereas supercooled water is observed at cloud top in these regions, the IFS convective parametrization by definition cannot produce much supercooled liquid at these cold temperatures. Modifying the diagnostic function to produce supercooled water at colder temperatures is one straightforward solution, but this also affects the deeper tropical convection, resulting in increased radiation biases due to an overprediction of supercooled liquid in the tropics. In fact the unique property of cloud tops at these temperatures is that there is a source of supercooled liquid, which is detrained from the strong convective updraughts, while the sink is primarily through the process of ice nucleation leading to slow glaciation over time. In deeper convection in the tropics there may already be significant frozen particles (snow or graupel) falling though the liquid, which acts to freeze or evaporate the drops, leading to less supercooled liquid water for the same temperature. The convection scheme therefore needs to capture this additional physics in order to differentiate between the deeper convective cloud with less supercooled liquid and the mid-level convective cloud with supercooled liquid present at cloud top.

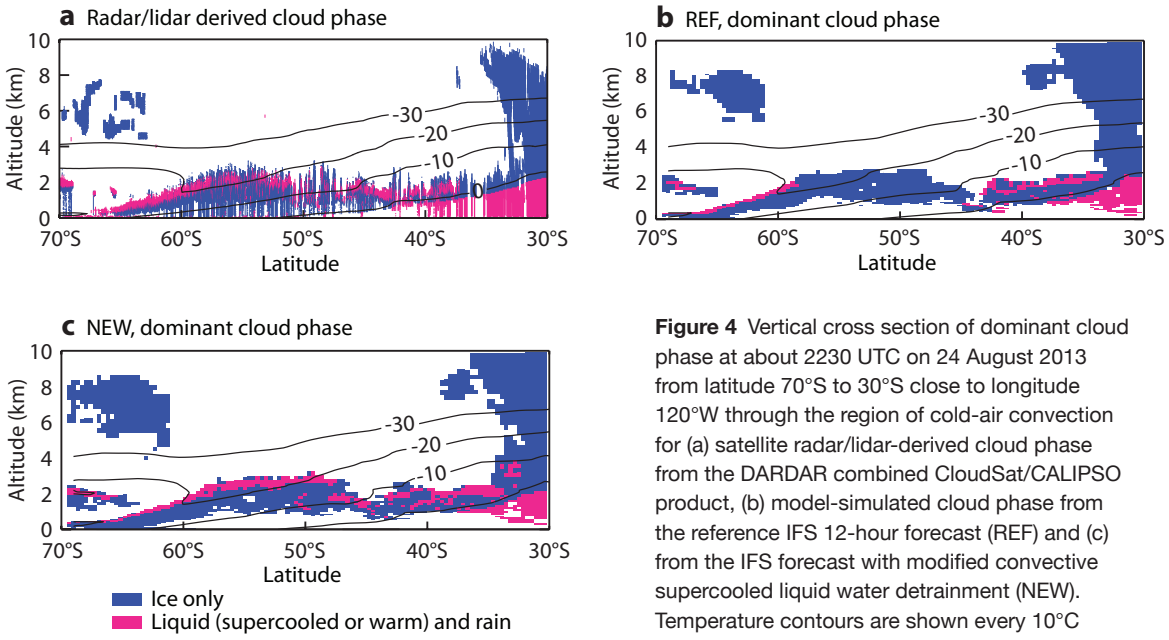

Figure 4 Vertical cross section of dominant cloud phase at about 2230 UTC on 24 August 2013 from latitude 70°S to 30°S close to longitude 120°W through the region of cold-air convection for (a) satellite radar/lidar-derived cloud phase from the DARDAR combined CloudSat/CALIPSO product, (b) model-simulated cloud phase from the reference IFS 12-hour forecast (REF) and (c) from the IFS forecast with modified convective supercooled liquid water detrainment (NEW). Temperature contours are shown every 10°C from 0° to -30°C.

doi:10.21957/s41h7q7l

To test the hypothesis, we performed a series of forecast experiments (NEW), equivalent to the reference (REF) but with modifications so that the convection produces all liquid condensate if the cloud top is below 600 hPa. For convective cloud tops higher than this the existing 0 to –23°C diagnostic phase function is used. Figure 3b,d,f shows the local impact in the Southern Ocean case study for liquid water path, microwave brightness temperature first guess departures and the shortwave radiation error. Liquid water is now present in the convective region where there were negligible amounts before; the 92 GHz first-guess departures are significantly reduced in the cold-air convection; and the shortwave radiation error is almost completely removed. The equivalent cross section to compare with the CloudSat/CALIPSO track across the convective region (Figure 4c) now shows the presence of supercooled liquid water in the cloud across the convective region and particularly at cloud top, in better agreement with the observed data.

The change also reduces the global time-mean bias in the shortwave radiation seen in Figure 1b. Figure 5a shows the annual mean top-of-atmosphere net shortwave radiation bias for a 1-year simulation of the IFS at the resolution of the seasonal prediction system (TL255, 80 km grid resolution). Although not exactly the same, the bias in this 1-year forecast at low resolution is remarkably similar to the 24-hour forecast bias at the operational 16 km grid resolution (Figure 1b), showing the robustness of the shortwave radiation systematic errors across scales. Figure 5b shows the impact of the modifications to the parametrization of convective supercooled liquid water. There is indeed a marked reduction in the shortwave bias, not only across the Southern Ocean, but also in the poleward storm track regions of the North Atlantic and North Pacific Oceans. Early results suggest a similar improvement for the higher-resolution model.

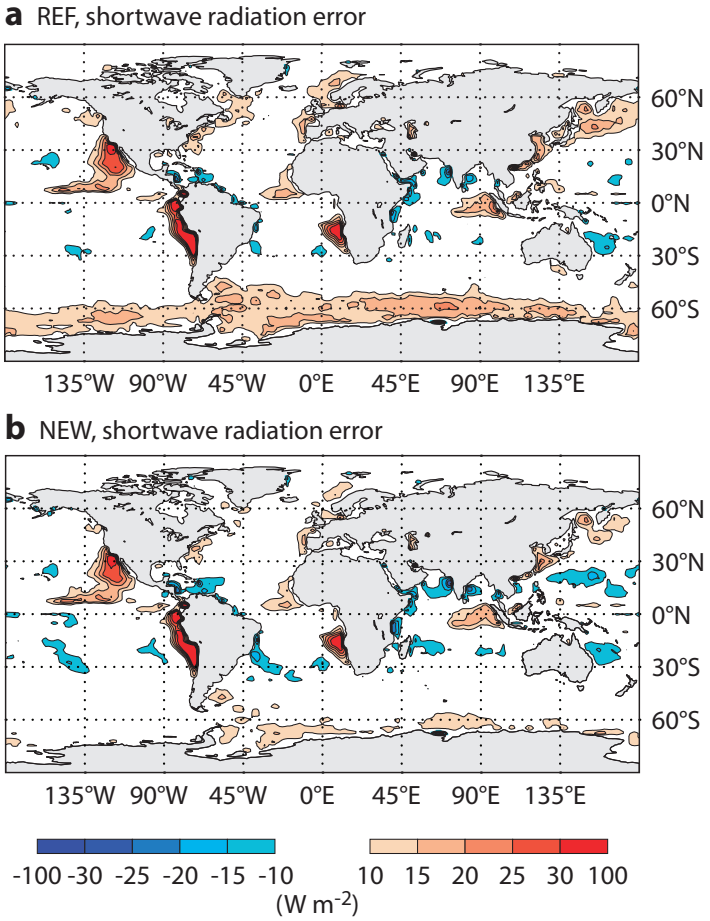

Figure 5 Difference between annual (2000–2001) mean top-of-atmosphere net shortwave radiation over the ocean in a 1-year IFS simulation at the resolution of the seasonal forecasting system (TL255) and in CERES satellite observations for (a) the reference IFS (REF) and (b) the IFS with the modified convective supercooled liquid water detrainment (NEW). The systematic error in the North Atlantic, North Pacific and Southern Ocean storm tracks is significantly reduced.

doi:10.21957/s41h7q7l

Summary and outlook

This article describes an example of using the data assimilation system to help to identify a regime-dependent systematic error in the model that can be linked to a specific parametrized process. An evaluation of the microwave radiance brightness temperature first-guess departures, combined with shortwave radiation and radar/lidar data from satellites, pointed to a lack of supercooled liquid water in the modelling of convective cold-air outbreaks in both hemisphere storm tracks. It is this combination of data sources that made it possible to identify the problem in the model and, importantly, to provide quantifiable information on the magnitude of the error. A solution that increases the detrained supercooled liquid water for convective updraughts with mid-level (below 600 hPa) cloud tops, which can be colder than –20°C, improves the first-guess fit to microwave radiances in the data assimilation scheme and the model impact of cloud on shortwave radiation. The long-standing shortwave radiation bias over the Southern Ocean, North Atlantic and North Pacific, seen at all IFS model resolutions and timescales from a few hours to seasonal timescales, is significantly reduced.

More work is required to assess the seasonal cycle of the errors and to implement a more physically based solution in the operational model. It will be important to assess downstream impacts of the reduction in these systematic errors, particularly on the sea-surface temperature in the coupled atmosphere–ocean configurations of the IFS.

Further reading

Bauer, P., A. J. Geer, P. Lopez & **D. Salmond,** 2010: Direct 4D-Var assimilation of all-sky radiances. Part I: Implementation. *Q.J.R. Meteorol. Soc.,* **136**, 1868–1885.

Forbes, R. M. & **M. Ahlgrimm,** 2014: On the representation of high-latitude boundary layer mixed-phase cloud in the ECMWF global model. *Mon. Wea. Rev.,* **142,** 3425–3445.

Forbes, R. & **A. Tompkins,** 2011: An improved representation of cloud and precipitation. *ECMWF Newsletter* **No. 129,** 13–18.

Geer, A. J. & **P. Bauer,** 2010: Enhanced use of all-sky microwave observations sensitive to water vapour, cloud and precipitation, *ECMWF Technical Memorandum* **No. 620.**

Hu, Y., S. Rodier, K.-M. Xu, W. Sun, J. Huang, B. Lin, P. Zhai & **D. Josset,** 2010: Occurrence, liquid water content and fraction of supercooled water clouds from combined CALIOP/IIR/MODIS measurements. *J. Geophys. Res.,* **115** (D4), D00H34.

Lonitz, K. & **A. Geer,** 2015: New screening of cold-air outbreak regions used in 4D-Var all-sky assimilation, *EUMETSAT/ECMWF Fellowship Programme Research Reports* **No. 35.**

© Copyright 2016

European Centre for Medium-Range Weather Forecasts, Shinfield Park, Reading, RG2 9AX, England

The content of this Newsletter article is available for use under a Creative Commons Attribution-Non-Commercial-No-Derivatives-4.0-Unported Licence. See the terms at https://creativecommons.org/licenses/by-nc-nd/4.0/.

The information within this publication is given in good faith and considered to be true, but ECMWF accepts no liability for error or omission or for loss or damage arising from its use.

doi:10.21957/s41h7q7l